

## Article

# Synergistic Combination of Irinotecan and Rapamycin Orally Delivered by Nanoemulsion for Enhancing Therapeutic Efficacy of Pancreatic Cancer

Yu-Hsuan Liu <sup>1,†</sup>, Ling-Chun Chen <sup>2,†</sup>, Wen-Ting Cheng <sup>2,†</sup>, Pu-Sheng Wei <sup>1</sup>, Chien-Ming Hsieh <sup>1</sup> , Ming-Thau Sheu <sup>1</sup> , Shyr-Yi Lin <sup>3,4</sup>, Hsiu-O Ho <sup>1,\*</sup> and Hong-Liang Lin <sup>5,\*</sup>

<sup>1</sup> School of Pharmacy, College of Pharmacy, Taipei Medical University, Taipei 11031, Taiwan

<sup>2</sup> Department of Biotechnology and Pharmaceutical Technology, Yuanpei University of Medical Technology, Hsinchu 30015, Taiwan

<sup>3</sup> Division of Gastroenterology, Department of Internal Medicine, Wan Fang Hospital, Taipei Medical University, Taipei 11696, Taiwan

<sup>4</sup> Department of General Medicine, School of Medicine, College of Medicine, Taipei Medical University, Taipei 11031, Taiwan

<sup>5</sup> School of Pharmacy, College of Pharmacy, Kaohsiung Medical University, Kaohsiung 80708, Taiwan

\* Correspondence: hsiuoho@tmu.edu.tw (H.-O.H.); hlglin@kmu.edu.tw (H.-L.L.)

† These authors contributed equally to this work.

**Abstract:** In recent years, combining different types of therapy has emerged as an advanced strategy for cancer treatment. In these combination therapies, oral delivery of anticancer drugs is more convenient and compliant. This study developed an irinotecan/rapamycin-loaded oral lecithin-based self-nanoemulsifying nanoemulsion preconcentrate ( $LB\text{SNENP}_{ir/ra}$ ) and evaluated its synergistic combination effects on pancreatic cancer.  $LB\text{SNENP}$  loaded with irinotecan and rapamycin at a ratio of 1:1 ( $LB\text{SNENP}_{ir10/ra10}$ ) had a better drug release profile and smaller particle size (<200 nm) than the drug powder. Moreover,  $LB\text{SNENP}_{ir10/ra10}$  exhibited a strong synergistic effect (combination index [CI] < 1.0) in cell viability and combination effect studies. In the tumor inhibition study, the antitumor activity of  $LB\text{SNENP}_{ir10/ra10/sily20}$  against MIA PaCa-2 (a human pancreatic cancer cell line) was significantly increased compared with the other groups. When administered with rapamycin and silymarin, the area under the curve and the maximum concentration of irinotecan significantly improved compared with the control. We successfully developed an irinotecan/rapamycin-loaded oral self-nanoemulsifying nanoemulsion system to achieve treatment efficacy for pancreatic cancer.

**Keywords:** irinotecan; rapamycin; silymarin; combination therapy; self-nanoemulsifying nanoemulsion; oral nano pharmaceuticals



**Citation:** Liu, Y.-H.; Chen, L.-C.; Cheng, W.-T.; Wei, P.-S.; Hsieh, C.-M.; Sheu, M.-T.; Lin, S.-Y.; Ho, H.-O.; Lin, H.-L. Synergistic Combination of Irinotecan and Rapamycin Orally Delivered by Nanoemulsion for Enhancing Therapeutic Efficacy of Pancreatic Cancer. *Pharmaceutics* **2023**, *15*, 473. <https://doi.org/10.3390/pharmaceutics15020473>

Academic Editors: Dumitru Lupuliasa, Emma Adriana Ozon and Anca Lucia Pop

Received: 11 November 2022

Revised: 16 December 2022

Accepted: 20 January 2023

Published: 31 January 2023



**Copyright:** © 2023 by the authors. Licensee MDPI, Basel, Switzerland. This article is an open access article distributed under the terms and conditions of the Creative Commons Attribution (CC BY) license (<https://creativecommons.org/licenses/by/4.0/>).

## 1. Introduction

Pancreatic adenocarcinoma (PAC) is a highly fatal malignancy with a five-year overall survival rate of 9% irrespective of the disease stage [1,2]. PAC is the fourth leading cause of cancer-related death in the United States, resulting in an estimated 45,750 deaths each year [2]. Although surgery is the primary treatment option for long-term survival, less than 20% of patients with PAC qualify for initial resection at diagnosis [3]. For patients with unresectable PAC, especially metastatic PAC, chemotherapy is essential for prolonging life expectancy. However, first-line systemic chemotherapy with 5-fluorouracil- or gemcitabine-based regimens slightly prolongs the overall survival of patients with metastatic PAC. The propensity of PAC to develop chemoresistance and the highly malignant behavior of PAC have substantially reduced treatment effectiveness for this disease [4].

Concurrent treatment has been taken as the key measure of treating cancer due to its primary advantages of maximizing the efficacy and minimizing the toxicity at an adequate ratio. Combination chemotherapy regimens involving leucovorin, fluorouracil,

irinotecan, oxaliplatin (FOLFIRINOX), and gemcitabine (GEM) plus nab-paclitaxel or erlotinib (Tarceva), have been demonstrated to improve the outcomes of patients with PAC [4–6]. Thus, FOLFIRINOX is among the primary standard treatments for unresectable PAC, and GEM plus nab-paclitaxel or erlotinib is another standard treatment option for PAC. Although combination therapies show better survival rate and quality of life (QoL), the overall improvement remains limited for advanced disease. Thus, effective strategies, new single agents, or new combination therapies are urgently required to markedly improve the clinical outcomes of patients with PACs.

The mammalian target of rapamycin (mTOR) signaling acts as the major regulator for cell proliferation. In the study, the patients with PAC and relatively high active phosphorylated mTOR<sup>S2448</sup> showed significantly shorter survival and account for 15–20% [7]. Therefore, targeted mTOR treatment may have positive impact on clinical outcomes from patients carrying PAC. The mTOR-dependent signals stimulated hypoxia-inducible factor-1 (HIF-1) $\alpha$  accumulation and HIF-1-mediated transcription in cells with hypoxic conditions [8]. HIF-1 acts as the main regulator for inducing vascular endothelial growth factor in a hypoxia situation [9]. The majority characterization of PACs is surrounded by a hypoxic tumor microenvironment [10,11]. Hypoxic tumors are more aggressive than oxygenated tumors [12–14]. Suppression of the mTOR-HIF-1 signaling pathway might therefore be an effective therapeutic strategy for PAC.

Irinotecan exhibits antiangiogenic properties. The mTOR inhibitor, rapamycin, targeted the mTOR-HIF-1 $\alpha$  axis and induced colon cancer cells to become sensitive to irinotecan, both in vitro and in vivo study using a xenografted metastasis model of human colorectal cancer. Moreover, low dose combinations made a significant portion of the tumor shrink, even in specimens resistant to irinotecan alone [15]. In a cytotoxicity study, the combination of irinotecan and rapamycin exerted a stronger killing effect on PSN1 cells between 48 and 72 h after incubation compared with irinotecan or rapamycin alone [16]. Jannier et al. reported that targeting the central node of the mTOR-HIF-1 axis with rapamycin and irinotecan suppressed the proliferation and metabolism of tumor cells [17]. Furthermore, Suzuki et al. demonstrated that the suppression of mTOR-HIF-1 signaling mediated the antitumor activity of metformin for PAC, revealing the different underlying mechanism from that of GEM. These results imply that the combination of rapamycin and irinotecan might be an effective therapeutic drug for PAC [18].

Currently, irinotecan is mainly administered through an intravenous bolus injection. Despite the advantages of oral chemotherapy over intravenous dosing [19,20], poor solubility and limited GI absorption can make oral therapy challenging. In the lumen of the gastrointestinal tract, oral bioavailability is often limited by the expression of ABC efflux transporters, such as P-glycoprotein (P-gp) and other metabolizing enzymes, including cytochrome P450 3A (CYP3A). Other limiting factors include the secretion from liver into bile via P-gp (ABCB1), the ATP-binding cassette drug-transporter C2 (ABCC2) and ATP-binding cassette drug-transporter G2 (ABCG2), and the first-pass effect in the liver [21–24]. In a previous study [24], the oral delivery of irinotecan was loaded in a self-emulsifying drug delivery system (SMEDDS) to enhance its solubility in combination with a P-gp/CYP3A dual-function inhibitor which was used to overcome the first-pass effect and increase the formation of the active metabolite SN-38. This method enhanced the antitumor effect due to the improved oral bioavailability of irinotecan, which made the active metabolite SN-38 form and accumulate.

In previous studies, a lecithin-based self-nanoemulsifying nanoemulsion preconcentrate (<sub>LB</sub>SNENP) was developed for the simultaneous loading of irinotecan and rapamycin with silymarin. This was used as the dual-function inhibitor for the oral delivery of the resultant self-nanoemulsifying nanoemulsion (<sub>LB</sub>SNENA) as a means of enhancing oral bioavailability [25–28]. We used this system and optimized it in the present study. Furthermore, most of the SMEDDSs used in this study, such as <sub>LB</sub>SNENA, are thermodynamically stable liquid formulations which demonstrated the high solubilization capacity of poorly

soluble drugs. Thus, they can be directly filled into soft or hard gelatin capsules and act as a convenient method of oral administration.

## 2. Materials and Methods

### 2.1. Materials

Silymarin (80%) was purchased from Sanjaing (Jiaxing, China). Irinotecan hydrochloride and SN-38 were purchased from Scino Pharm (Tainan, Taiwan). SN38G was purchased from Cayman Chemical (Ann Arbor, MI, USA). Rapamycin was purchased from Chunghwa Chemical Synthesis and Biotech (New Taipei City, Taiwan). Capryol-90 was purchased from Gattefosse (Lyon, France). Tween 80 and camptothecin were purchased from Merck KGaA (Darmstadt, Germany). Cremophor EL was procured from Wei Ming Pharmaceutical (Taipei, Taiwan). Ascomycin was purchased from MedChemExpress (South Brunswick, NJ, USA). Soybean lecithin (Lipoid S-100) was purchased from Lipoid GmbH (Ludwigshafen, Germany). Dulbecco's modified Eagle's medium, fetal bovine serum, and horse serum were purchased from Corning (New York, NY, USA). Reagents used for high-performance liquid chromatography (HPLC) or ultra-performance liquid chromatography with tandem mass spectrometry (UPLC/MS/MS) were of HPLC or MS grade, and other reagents were of analytical grade.

### 2.2. Preparation of Irinotecan/Rapamycin-Loaded $_{LB}SNENP$

Based on the results of previous studies, a mixture of lecithin and Tween 80 with cremophor EL as the surfactant system (SAA), and capryol-90 was selected as the oil phase, and propylene glycol (PG) as the cosurfactant [23]. Irinotecan/rapamycin-loaded oral  $_{LB}SNENP$  was prepared using 18% capryol-90, 58% SAA, and 24% w/w PG with the drugs. These two drugs simultaneously dissolved in  $_{LB}SNENP$  and formed an opalescent/translucent nanoemulsion. The irinotecan or rapamycin content was 10 mg in 1 g of  $_{LB}SNENP$ . The mixture was heated in a 50–60 °C water bath until it completely dissolved into a light yellow and clear solution. Table 1 revealed the composition of 1 g of  $_{LB}SNENP_{bk}$ ,  $_{LB}SNENP_{ir10}$ , and  $_{LB}SNENP_{ra10}$ .

**Table 1.** Composition of 1 g  $_{LB}SNENP_{bk}$ ,  $_{LB}SNENP_{ir10}$ , and  $_{LB}SNENP_{ra10}$ .

Formulations	Drug		Oil (18%)	Co-Surfactant (24%)	Surfactants (58% SAA)		
	Irinotecan	Rapamycin	Capryol 90	Propylene glycol	Lecithin	Tween 80	Cremophor EL
$_{LB}SNENP_{bk}$	-	-	0.182 g	0.242 g	0.198 g	0.286 g	0.092 g
$_{LB}SNENP_{ir10}$	10 mg	-	0.182 g	0.242 g	0.198 g	0.286 g	0.092 g
$_{LB}SNENP_{ra10}$	-	10 mg	0.182 g	0.242 g	0.198 g	0.286 g	0.092 g

Abbreviations:  $_{LB}SNENP$ , lecithin-based self-nanoemulsifying nanoemulsion; bk, blank; ir, irinotecan; ra, rapamycin; number is dose.

### 2.3. Characterization of Irinotecan/Rapamycin-Loaded $_{LB}SNENP$

In this study, 100  $\mu$ L of  $_{LB}SNENP_{bk}$ ,  $_{LB}SNENP_{ir10}$ , and  $_{LB}SNENP_{ra10}$  was separately added to a 20-mL sample bottle containing 10 mL of double-distilled water. Then, the solution was gently shaken to obtain  $_{LB}SNENP_{bk}$ ,  $_{LB}SNENP_{ir10}$ , and  $_{LB}SNENP_{ra10}$ , respectively. The average droplet size and size distribution of each formulation were measured at 25 °C by using an N5 submicron particle size analyzer (Beckman Coulter, Brea, CA, USA) at a scattering angle of 90°, and the intensity autocorrelation of the sample ranged from  $5 \times 10^4$  to  $1 \times 10^6$ . Measurements were conducted three times for all the formulations to calculate the average diameter (nm), polydispersity index (PDI) and zeta potential (mV). The stability of  $_{LB}SNENP_{bk}$ ,  $_{LB}SNENP_{ir10}$ , and  $_{LB}SNENP_{ra10}$  was evaluated at room temperature for 1 month. At each time point, some samples were collected to determine the droplet size and the contents of irinotecan and rapamycin.

#### 2.4. HPLC Instrumentation and Chromatographic Conditions

The contents of irinotecan and rapamycin in  ${}_{LB}SNENP_{ir}$  and  ${}_{LB}SNENP_{ra}$  were detected through HPLC. To determine the irinotecan content, we used the Waters 600E HPLC system with the SunFire C18 column (4.6 mm  $\times$  250 mm I.D., 5  $\mu$ m; Waters). The mobile phase consisted of 10 mM phosphate buffer (pH 3.0)/acetonitrile/tetrahydrofuran (65/35/2 *v/v*), the flow rate was 0.8 mL/min, the column was maintained at 40  $^{\circ}$ C, the injection volume was 20  $\mu$ L, and the fluorescence detector was set at the excitation and emission wavelengths of 370 and 470 nm, respectively. To determine the rapamycin content, we used the JASCO HPLC system with the Inersil ODS-2 C18 column (4.0 mm  $\times$  150 mm I.D., 5  $\mu$ m). The mobile phase was a mixture of acetonitrile and water (20/80 *v/v*), the flow rate was 1.0 mL/min, the column was maintained at 55  $^{\circ}$ C, the injection volume was 100  $\mu$ L, and the UV detector was set at the wavelength of 278 nm. Each data point came from the mean of at least three individual trials. The assay method was also well validated before. Analytical graphs are provided in the supplemental information, Supplementary Material Figures S1 and S2.

#### 2.5. Simultaneous Analysis of Irinotecan, SN38, SN38 Glucuronide, and Rapamycin in the Biosample through Ultra-Performance Liquid Chromatography with Tandem Mass Spectrometry

Chromatography was performed using a Waters Xevo TQ-XS with an Acquity UPLC system. Separation was performed using an Acquity UPLC BEH C18 column (2.1  $\times$  100 mm I.D., 1.7  $\mu$ m; Waters). The column was maintained at 55  $^{\circ}$ C, and the autosampler was set at 4  $^{\circ}$ C. The injection volume was 2  $\mu$ L. Mobile phase A was 10 mM ammonium acetate (pH 3.0), and mobile phase B was acetonitrile. The gradient conditions of mobile phase B were as follows: 10% of mobile phase B for the first 1 min at a flow rate of 0.4 mL/min; mobile phase B was then linearly increased to 70% for 2 min and maintained for 1 min, and increased to 100% in 0.1 min at a flow rate of 0.7 mL/min and maintained for 1.5 min; the system finally returned to the initial condition in 2 min. The multiple reaction monitoring (MRM) scan mode was used for the quantification of the analytes irinotecan, SN38, SN38 glucuronide (SN38G), and rapamycin as well as the internal standards, camptothecin and ascomycin. Table 2 lists the protonated parents of the MS2 fragment ion MRM transitions for quantitation. The MS/MS instrument was operated using electrospray ionization in the positive mode, and the optimized parameters were as follows: desolvation temperature, 500  $^{\circ}$ C; source temperature, 150  $^{\circ}$ C; capillary voltage, 3.0 kV; cone gas flow, 150 L/h; and desolvation gas flow, 1000 L/h. Analytical graphs are provided in the supplemental information.

**Table 2.** Optimized MRM parameters of irinotecan, SN38, SN38G, rapamycin, camptothecin, and ascomycin.

Compounds	Formula	Parent <i>m/z</i>	Daughters <i>m/z</i>	Cone Volt.	Col. Energy
Irinotecan	C <sub>33</sub> H <sub>38</sub> N <sub>4</sub> O <sub>6</sub>	587.31	124.10	76	34
SN38	C <sub>22</sub> H <sub>20</sub> N <sub>2</sub> O <sub>5</sub>	393.21	349.14	70	26
SN38G	C <sub>28</sub> H <sub>28</sub> N <sub>2</sub> O <sub>11</sub>	569.20	393.17	78	28
Rapamycin	C <sub>51</sub> H <sub>79</sub> NO <sub>13</sub>	931.60	864.50	35	16
Camptothecin	C <sub>20</sub> H <sub>16</sub> N <sub>2</sub> O <sub>4</sub>	349.14	305.15	52	22
Ascomycin	C <sub>43</sub> H <sub>69</sub> NO <sub>12</sub>	809.51	756.49	48	22

Note: the analytes are irinotecan, SN38, SN38 glucuronide (SN38G), and rapamycin. The internal standards are camptothecin and ascomycin.

#### 2.6. In Vitro Release of Irinotecan and Rapamycin from ${}_{LB}SNENP$

The in vitro release of irinotecan and rapamycin from  ${}_{LB}SNENP$  was examined using the dissolution method on United States Pharmacopeia (USP) Apparatus 2 (VK7000, Vankel, UK). The release medium of irinotecan was 500 mL of buffer (pH 1.2). The release medium of rapamycin was 0.4% sodium lauryl sulfate solution. The temperature of the dissolution medium was maintained at 37  $^{\circ}$ C  $\pm$  0.5  $^{\circ}$ C. The stirring rates for irinotecan and rapamycin were 50 and 100 rpm, respectively. Briefly, 3-mL aliquots of the sample were withdrawn for the assay at predetermined time points (0, 5, 10, 15, 30, 45, and 60 min) and replaced with

the identical volume of the fresh medium. The contents of irinotecan and rapamycin were determined through HPLC as described in the earlier text. We filled 0.1 g of the irinotecan and rapamycin (10 mg/g) from  $_{LB}SNENP$  in number 0 empty hard capsules. Two control groups were the irinotecan and rapamycin powder. Each dissolution data point was the mean of at least three individual trials.

### 2.7. Cell Viability and Combination Effect Studies

To evaluate the cytotoxicity and combination effects of rapamycin and silymarin as well as free irinotecan, we performed the 3-(4,5-dimethylthiazol-2-yl)-2,5-diphenyl-2H-tetrazolium bromide (MTT) assay by using the MIA PaCa-2 pancreatic cancer cell line. Briefly, the cells were seeded in a 96-well plate at a density of  $3 \times 10^4$  cells/well and incubated at 37 °C with 5% CO<sub>2</sub> for 24 h. After 24 h, the cells were treated with different concentrations of free irinotecan (0–300 μM), rapamycin (0–300 μM), SN38 (0–300 nM), and silymarin (0–1000 μM). To determine the combination effect, the cells were treated with different ratios of irinotecan/rapamycin and SN38/rapamycin (1/0.3, 1/0.5, 1/1, and 1/2) and irinotecan/silymarin and SN38/silymarin (1/1 and 1/2). All the cells were incubated with the drugs for 24–48 h. Then, the MTT reagent and dimethyl sulfoxide were added for the formation and the dissolution of purple formazan crystals. The absorbance of each well was measured at 550 nm on a Cytation 3 cell imaging multimode reader (BioTek, Winooski, VT, USA). The half-maximal inhibitory concentration (IC<sub>50</sub>) and combination index (CI) of the drugs were calculated using CompuSyn Software (Paramus, NJ, USA) through the Chou–Talalay method. In the Chou–Talalay method, the CI values of <0.9, >1.1, and 0.9–1.1 indicated synergistic, antagonistic, and additive effects, respectively. Each data point was the mean of at least six individual experiments.

### 2.8. In Vivo Pharmacokinetic Studies

All animal experiments followed the protocol approved by the Laboratory Animal Center of Taipei Medical University (Approval No: LAC-2017-0334) and were conducted in compliance with the Animal Welfare Act. Eight-week-old male Sprague Dawley rats were used to investigate the pharmacokinetic (PK) profiles of irinotecan, SN38, SN38G, and rapamycin after single-dose oral administration. In total, 40 rats were randomized into eight groups (n = 5 per group): irinotecan solution in water (Sol<sub>ir10</sub>), rapamycin solution in water (Sol<sub>ra10</sub>),  $_{LB}SNENP_{ir10}$ ,  $_{LB}SNENP_{ra10}$ ,  $_{LB}SNENP_{ir10/ra5}$ ,  $_{LB}SNENP_{ir10/ra10}$ ,  $_{LB}SNENP_{ir10/ra5/sily20}$ , and  $_{LB}SNENP_{ir10/ra10/sily20}$ . Table 3 lists the dosing from different groups. All blood samples from the jugular vein were collected into K<sub>2</sub>EDTA blood collection tubes at 0.0833, 0.5, 1, 2, 3, 4, 6, 8, 10, 12, and 24 h after oral administration and were then stored at 4 °C. Next, 300 μL of the blood samples were added to 1.5-mL microtubes and immediately centrifuged at 6000 rpm for 10 min at 4 °C to obtain plasma. The plasma samples were stored at –80 °C until UPLC/MS/MS. PK parameters were calculated through a noncompartmental analysis using WinNonlin software (Pharsight, Princeton, NJ, USA). The results are expressed as mean ± standard deviation (SD). Relative bioavailability (F<sub>RB</sub>) was calculated using the following equation:

$$F_{RB} = \frac{AUC_A/dose_A}{AUC_B/dose_B} \times 100\%$$

**Table 3.** The dose of irinotecan, rapamycin, and silymarin in each group of PK studies.

Dose	1 g dd H <sub>2</sub> O		1 g LB SNENP					
	Sol <sub>ir10</sub>	Sol <sub>ra10</sub>	LB SNENP <sub>ir10</sub>	LB SNENP <sub>ra10</sub>	LB SNENP <sub>ir10/ra5</sub>	LB SNENP <sub>ir10/ra10</sub>	LB SNENP <sub>ir10/ra5/sily20</sub>	LB SNENP <sub>ir10/ra10/sily20</sub>
Irinotecan (mg/kg)	10	-	10	-	10	10	10	10
Rapamycin (mg/kg)	-	10	-	10	5	10	5	10
Silymarin (mg/kg)	-	-	-	-	-	-	20	20

Abbreviations: Sol, solution; LB SNENP, lecithin-based self-nanoemulsifying nanoemulsion preconcentrate; ir, irinotecan; ra, rapamycin; sily, silymarin; number is dose.

### 2.9. Bioanalysis of the Blood Concentrations of Irinotecan, SN-38, SN38G, and Rapamycin

To extract irinotecan, SN-38, and SN38G from the plasma samples, 100 µL of the plasma sample was mixed with 200 µL of acetonitrile for 3 min by using a multitube vortexer to extract analytes. After 6000-rpm centrifugation for 10 min at 4 °C, 0.1 mL of the supernatant was transferred to another 1.5-mL microtube and stored at 4 °C (analyte A). Subsequently, to collect rapamycin, 200 µL of the extracted solution (methanol/0.1 M zinc sulfate solution = 7/3) was added to 100 µL of the blood sample and vortexed for 1 min. The mixture was centrifuged at 6000 rpm at 4 °C for 10 min, and 100 µL of the supernatant was mixed with analyte A and vortexed for 10 s (analyte B). Subsequently, 10 µL of camptothecin (1 µg/mL) and 10 µL of ascomycin (3 µg/mL) were added to analyte B and then diluted with the mobile phase and mixed thoroughly. The final sample solution was injected into the UPLC/MS/MS system for analysis.

### 2.10. Tumor Inhibition Studies

All animal experiments followed the protocol approved by the Laboratory Animal Center of Taipei Medical University (Approval No: LAC-2017-0334) and were performed following animal care guidelines. Five-week-old male nu/nu mice received a subcutaneous injection of 100 µL (containing  $15 \times 10^5$  cells) of a MIA PaCa-2 cell suspension in Matrigel into their back. These tumor-bearing mice with a tumor volume of approximately 100 mm<sup>3</sup> were randomized into seven groups: one control group (saline) and six experimental groups, namely LB SNENP<sub>ir10</sub>, LB SNENP<sub>ra10</sub>, LB SNENP<sub>ir10/ra5</sub>, LB SNENP<sub>ir10/ra10</sub>, LB SNENP<sub>ir10/ra5/sily20</sub>, and LB SNENP<sub>ir10/ra10/sily20</sub> (n = 3–5 per group). Table 4 lists the dosing from different groups. Each formulation was orally administered 4 times every 3 days. The tumor volumes and body weights of the mice were measured every 3 days after the administration of the formulations. The tumor volume was calculated using the formula  $1/2 \text{ length} \times \text{width}^2$ . The mice were sacrificed through CO<sub>2</sub> inhalation, and the tumors were harvested and weighed on day 31. The tumor growth inhibition rate (TGI%) was calculated as follows:  $(W_c - W_t)/W_c$ , where  $W_t$  is the tumor weight of each formulation group, and  $W_c$  is the tumor weight of the control group [23].

**Table 4.** The dose of irinotecan, rapamycin, and silymarin in each group of efficacy studies.

Dose	Groups						
	Saline	LB SNENP <sub>ir10</sub>	LB SNENP <sub>ra10</sub>	LB SNENP <sub>ir10/ra5</sub>	LB SNENP <sub>ir10/ra10</sub>	LB SNENP <sub>ir10/ra5/sily20</sub>	LB SNENP <sub>ir10/ra10/sily20</sub>
Irinotecan (mg/kg)	-	10	-	10	10	10	10
Rapamycin (mg/kg)	-	-	10	5	10	5	10
Silymarin (mg/kg)	-	-	-	-	-	20	20

Abbreviations: LB SNENP, lecithin-based self-nanoemulsifying nanoemulsion preconcentrate; ir, irinotecan; ra, rapamycin; sily, silymarin; number is dose.

### 2.11. Statistical Analysis

Data are expressed as the mean  $\pm$  SD of each study. Significant differences among the samples were determined using one-way analysis of variance (ANOVA). *p* value of 0.05 indicated statistical significance.

## 3. Results and Discussion

### 3.1. Characterization of $_{LB}SNENA$

The optimized  $_{LB}SNENP$ , composed of capryol-90, SAA, and PG at a weight ratio of 18/58/24, was selected to encapsulate irinotecan and rapamycin to form  $_{LB}SNENA$ . These two drugs completely dissolved in  $_{LB}SNENP$ , forming an opalescent/translucent nanoemulsion. As presented in Table 5, the mean droplet size (nm) and PDI of  $_{LB}SNENA_{ir}$  and  $_{LB}SNENA_{ra}$  were  $122.7 \pm 1.84$  ( $0.212 \pm 0.011$ ) nm and  $120.8 \pm 2.25$  ( $0.224 \pm 0.010$ ) nm, respectively, which were similar to those of  $_{LB}SNENA_{bk}$  ( $149.3 \pm 2.48$  [ $0.305 \pm 0.043$ ] nm). The zeta potential (mV) of  $_{LB}SNENA_{ir}$  and  $_{LB}SNENA_{ra}$  were  $-4.14 \pm 0.24$  mV and  $-8.20 \pm 0.30$  mV, respectively, which were similar to those of  $_{LB}SNENA_{bk}$  ( $-7.32 \pm 0.46$  mV). The results indicated that the drugs loaded in  $_{LB}SNENP$  did not affect the self-nanoemulsifying property. Furthermore, during a 30-day period, the stability of the homogenous nanoemulsions of  $_{LB}SNENA_{ir}$  and  $_{LB}SNENA_{ra}$  was maintained at room temperature without precipitation, aggregation, or delamination. As presented in Figure 1A, the concentrations of irinotecan and rapamycin loaded in the nanoemulsions on day 30 did not differ from those on the initial day (>90%).

**Table 5.** The mean droplet size, PDI, and zeta potential of  $_{LB}SNENA$ .

Sample	Droplet Size (nm)	PDI	Zeta Potential (mV)
$_{LB}SNENA_{bk}$	$149.3 \pm 2.48$	$0.305 \pm 0.043$	$-7.32 \pm 0.46$
$_{LB}SNENA_{ir10}$	$122.7 \pm 1.84$	$0.212 \pm 0.011$	$-4.14 \pm 0.24$
$_{LB}SNENA_{ra10}$	$120.8 \pm 2.25$	$0.224 \pm 0.010$	$-8.20 \pm 0.30$

Abbreviations:  $_{LB}SNENA$ , lecithin-based self-nanoemulsifying nanoemulsion; bk, blank; ir, irinotecan; ra, rapamycin; number is dose.

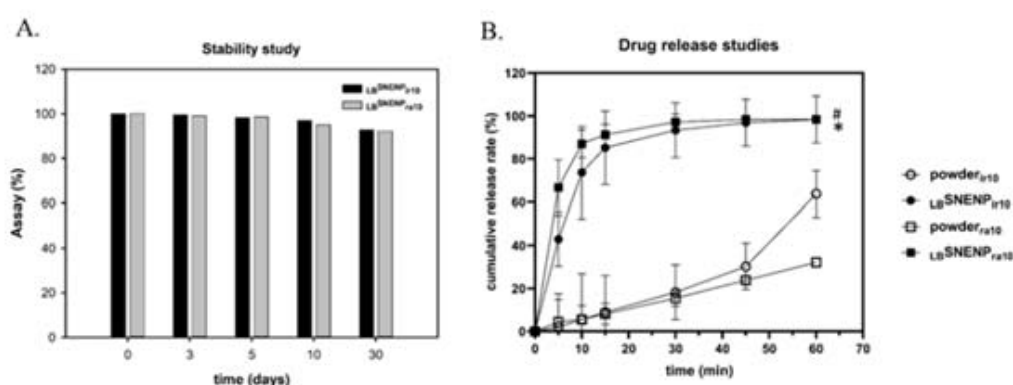


**Figure 1.** Content of irinotecan or rapamycin-loaded  $_{LB}SNENP$  in the stability test (A); drug release profiles of the irinotecan powder, rapamycin powder,  $_{LB}SNENP_{ir}$ , and  $_{LB}SNENP_{ra}$  (B). \* *p* < 0.05 when  $_{LB}SNENP_{ir}$  was compared with the irinotecan powder. # *p* < 0.05 when  $_{LB}SNENP_{ra}$  was compared with the rapamycin powder. Each point is shown as mean  $\pm$  standard deviation (*n* = 3). Abbreviations:  $_{LB}SNENP$ , lecithin-based self-nanoemulsifying nanoemulsion preconcentrate; powder is pure drug; ir, irinotecan; ra, rapamycin; number is dose.

### 3.2. In Vitro Release of Irinotecan and Rapamycin from $_{LB}SNENP$

The release of irinotecan and rapamycin (10 mg/g) from  $_{LB}SNENP$  was examined using the USP dissolution method, and the results are illustrated in Figure 1B. The cumulative release rates of irinotecan and rapamycin from  $_{LB}SNENP$  rapidly reached approximately 85% and 90%, respectively, at 15 min. Both the formulations were completely released within 30 min. The dissolution percentages of raw irinotecan and rapamycin powders were only approximately 63% and 32%, respectively, at the endpoint. Compared with the raw powders,  $_{LB}SNENP_{ir}$  and  $_{LB}SNENP_{ra}$  exhibited a significant difference in their dissolution percentages ( $p < 0.05$ ). The results indicate that  $_{LB}SNENP$  can considerably improve the solubility and release rate of hydrophobic drugs.

### 3.3. Cell Viability and Combination Effect Studies

Cell viability and combination effects were determined using the MTT assay. We evaluated the antitumor effects of irinotecan, SN38, rapamycin, and silymarin at different ratios on a human pancreatic cancer cell line (MIA PaCa-2). SN38 is an active metabolite of irinotecan, and its activity is approximately 100–1000 times that of irinotecan. Therefore, we designed the sample concentration range of irinotecan, rapamycin, and silymarin in micromolarity and that of SN38 in nanomolarity. The IC<sub>50</sub> values of irinotecan, SN38, rapamycin, and silymarin against MIA PaCa-2 cells were  $4.78 \pm 9.42$ ,  $51.71 \pm 33.41$ ,  $2.98 \pm 0.97$ , and  $216.73 \pm 32.78$   $\mu$ M, respectively, at 24 h and  $12.20 \pm 4.56$ ,  $50.74 \pm 10.64$ ,  $3.88 \pm 1.17$ , and  $153.08 \pm 34.13$   $\mu$ M, respectively, at 48 h.

To investigate combination effects, we mixed rapamycin with 300  $\mu$ M irinotecan or 300 nM SN38 at different ratios (0.3:1, 0.5:1, 1:1, and 2:1). Subsequently, we combined silymarin with irinotecan or SN38 at the ratios of 1:1 and 1:2 and then serially diluted and co-delivered them to treat the cells. The results of rapamycin/irinotecan and rapamycin/SN38 treatments are presented in Table 6. The CI value of rapamycin/irinotecan ranged from 0.11 (concentration ratio = 0.3:1 at 24 h) to 0.28 (concentration ratio = 2:1 at 24 h). The CI value of rapamycin/SN38 at 24 h appeared to be similar to that of rapamycin/irinotecan. Except for irinotecan/silymarin at the ratio of 1:2, the CI value of silymarin combined with irinotecan or SN38 (1:1 or 1:2) was <1.0 at 24 h. After 48-h treatment, all the groups exhibited greater improvement in the inhibition of cell proliferation; thus, their CI values were <0.1. The results indicate that the aforementioned combinations are considerably effective against MIA PaCa-2 cells when  $_{LB}SNENP$  is used as the co-delivery system for irinotecan, rapamycin, and silymarin.

**Table 6.** Combination index (CI<sub>50</sub>) for different ratios of irinotecan, SN38, rapamycin, and silymarin at 24 and 48 h.

Drug	Ratio	CI <sub>50</sub>	
		24 h	48 h
rapamycin:irinotecan	0.3:1	0.11	0.02
	0.5:1	0.16	0.01
	1:1	0.10	0.07
	2:1	0.28	0.01
	0.3:1	0.20	0.01
rapamycin:SN38	0.5:1	0.21	0.04
	1:1	0.35	0.03
	2:1	0.23	0.04
irinotecan:silymarin	1:1	0.69	0.01
	2:1	1.44	0.00
	1:1	0.97	0.09
SN38:silymarin	2:1	0.84	0.14

### 3.4. In Vivo PK studies

The 8-week-old male Sprague Dawley rats with jugular vein catheters were used as the experimental animals. They were randomly divided into eight groups ( $n =$  five per group) and were administered the drugs once through oral gavage. The PK profiles and related PK parameters for irinotecan (Figure 2A and Table 7), SN38 (Figure 2B and Table 8), SN38G (Figure 2C and Table 9), and rapamycin (Figure 2D and Table 10) are illustrated in Figure 2 and listed in Tables 3–6, respectively. According to the irinotecan injection package insert, plasma samples would mainly comprise the prototype of irinotecan, followed by SN38G and SN38. In our studies, the results of the distribution of irinotecan, SN38G, and SN38 in plasma measured through UPLC/MS/MS were compatible with the data provided in the injection package insert. Notably, the pharmacokinetics parameters calculated for irinotecan and rapamycin showed the comparable trend of the maximum serum concentration ( $C_{max}$ ), which demonstrated that  $LB$ SNENP developed in this study obviously increased the absorption of irinotecan and rapamycin, resulting in the increase of  $C_{max}$  by approximately 2.0–5.7 and 3–10 times, respectively, compared with that of irinotecan and rapamycin aqueous solution ( $Sol_{ir10}$  and  $Sol_{ra10}$ , respectively). However,  $LB$ SNENP groups with rapamycin also exhibited the higher  $C_{max}$  values of irinotecan and SN38, compared with the  $LB$ SNENP group without rapamycin, which may be attributed to the combination of rapamycin. As previously reported, rapamycin inhibited the P-glycoprotein by competitive inhibition, which efficiently decreased the elimination of irinotecan [29]. Thus, increasing the amount of rapamycin evidently increased the area under the curve ( $AUC_{0 \rightarrow \infty}$ ) of irinotecan and SN38. SN38, a major active metabolite of irinotecan, is metabolized by carboxylesterases. Irinotecan was metabolized by the enzymes encoded by the UGT1A1 and CYP3A4 genes to form the inactive metabolites SN38G, APC, and NPC. Therefore, the increase in AUC of SN38 could lead to the better anticancer effect. Based on the area under the curve ( $AUC_{0 \rightarrow \infty}$ ) of  $Sol_{ir10}$ , the relative bioavailability ( $F_{RB}$ ) of irinotecan, SN38, and rapamycin loaded in  $LB$ SNENP was calculated using the formula previously described. The  $F_{RB}$  of irinotecan, SN38, and rapamycin was enhanced by approximately 2.0–5.0, 1.1–3.0, and 1.5–4.3 times, respectively. The conversion efficiency of SN38 is a key point in the efficiency of cancer therapy. The results of the conversion efficiency of SN38 are listed in Table 8. Irinotecan (10 mg/g), combined with rapamycin (10 mg/g) and silymarin (20 mg/g) loaded in  $LB$ SNENP, exhibited the highest value (75.2%), followed by  $LB$ SNENP $_{ir10/ra10}$  (61.9%). Although the  $F_{RB}$  of  $LB$ SNENP $_{ir10/ra10/sily20}$  was lower than that of  $LB$ SNENP $_{ir10/ra10}$ , the higher conversion efficiency might enhance the blood concentration of SN38 to improve antitumor efficacy. Furthermore, SN38G is the inactive metabolite of SN38 [30]. The values of  $C_{max}$  and AUC of SN38G in the  $LB$ SNENP groups with rapamycin were higher than those in the  $LB$ SNENP group without rapamycin, which resulted from the higher amount of SN38. In particular, the time in which maximum plasma concentration ( $T_{max}$ ) was reached was delayed significantly in those  $LB$ SNENP groups with rapamycin, indicating that the addition of rapamycin delayed the metabolism of SN38. This result was consistent with the previous report, which showed that the mTOR inhibitor could also act as UGT1A1 inhibitor [31].

In the PK study of rapamycin administered in combination with irinotecan and silymarin, the  $C_{max}$  and  $AUC_{0 \rightarrow \infty}$  of rapamycin showed gradual downward trends. These phenomena have been reported in the literature. When the P-gp inhibitor (rapamycin) was co-delivered with the chemotherapeutic reagent (irinotecan), it prevented the elimination of antitumor drugs and promoted the accumulation of drugs in the body. In conclusion, with the synergistic effects of P-gp and the mTOR inhibitor (rapamycin) and CYP3A4 inhibitor (silymarin), irinotecan loaded in  $LB$ SNENP increased the  $C_{max}$ ,  $AUC_{0 \rightarrow \infty}$ ,  $F_{RB}$ , and conversion efficiency of SN38; this might also improve the efficacy of combination therapy.

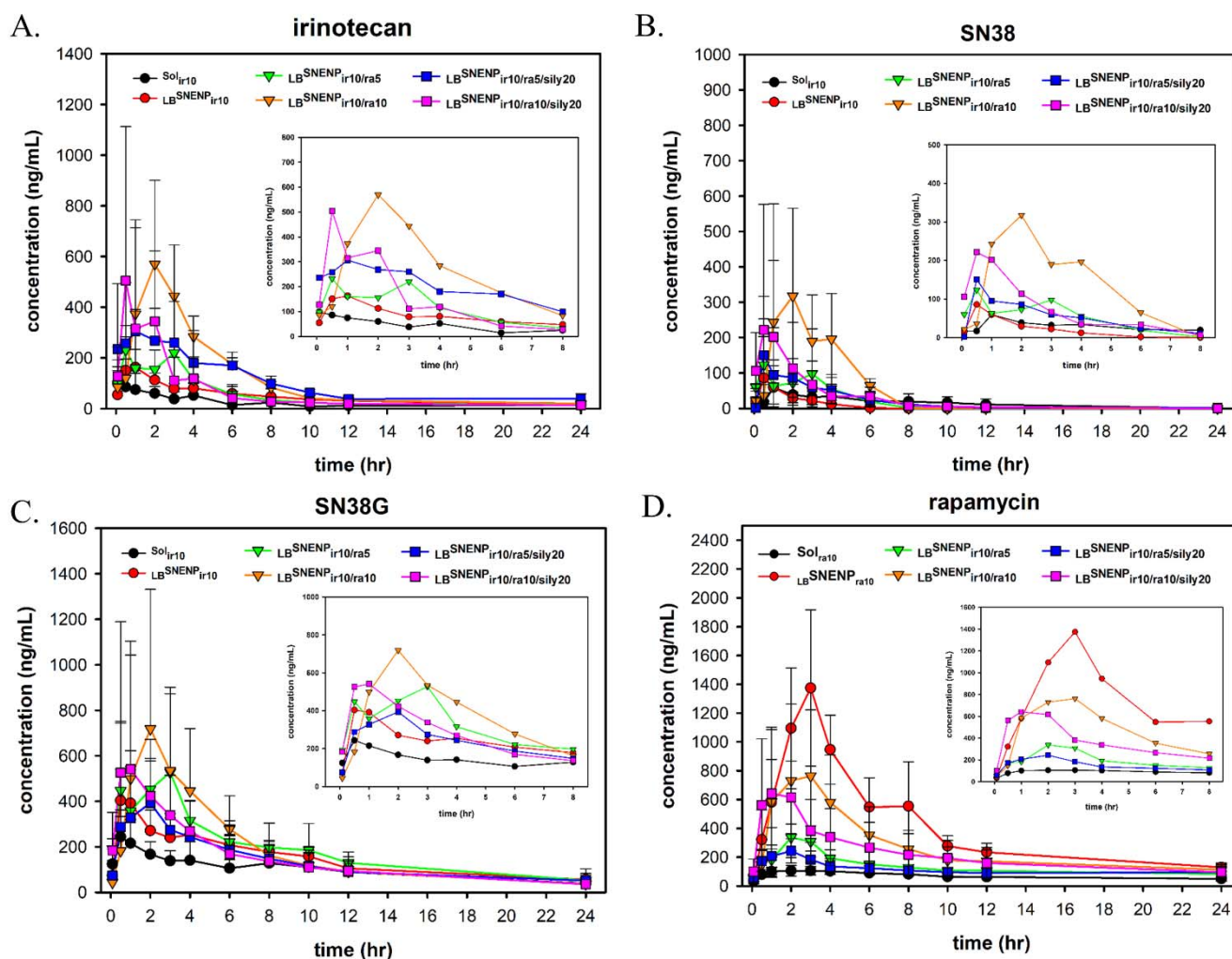


**Figure 2.** In vivo PK profiles of irinotecan (A), SN38 (B), SN38G (C), and rapamycin (D) after oral administration with Sol<sub>ir10</sub>, Sol<sub>ra10</sub>, LB<sup>SNENP</sup><sub>ir10</sub>, LB<sup>SNENP</sup><sub>ra10</sub>, LB<sup>SNENP</sup><sub>ir10/ra5</sub>, LB<sup>SNENP</sup><sub>ir10/ra10</sub>, LB<sup>SNENP</sup><sub>ir10/ra5/sily20</sub>, and LB<sup>SNENP</sup><sub>ir10/ra10/sily20</sub>. Each point is shown as mean  $\pm$  standard deviation ( $n = 3-5$ ). Abbreviations: Sol, solution; LB<sup>SNENP</sup>, lecithin-based self-nanoemulsifying nanoemulsion preconcentrate; ir, irinotecan; ra, rapamycin; sily, silymarin; number is dose.

**Table 7.** PK parameter estimations of irinotecan after oral administration with Sol<sub>ir10</sub>, LB<sup>SNENP</sup><sub>ir10</sub>, LB<sup>SNENP</sup><sub>ir10/ra5</sub>, LB<sup>SNENP</sup><sub>ir10/ra10</sub>, LB<sup>SNENP</sup><sub>ir10/ra5/sily20</sub>, and LB<sup>SNENP</sup><sub>ir10/ra10/sily20</sub>.

Title	Sol		LB <sup>SNENP</sup>			
	ir10	ir10	ir10/ra5	ir10/ra10	ir10/ra5/sily20	ir10/ra10/sily20
$C_{max}$ (ng/mL)	106.4 $\pm$ 86.6	205.3 $\pm$ 86.6	349.7 $\pm$ 257.8	606.2 $\pm$ 283.6	360.1 $\pm$ 104.0	576.5 $\pm$ 497.0
$T_{max}$ (h)	1.2 $\pm$ 1.6	1.2 $\pm$ 0.8	2.1 $\pm$ 1.2	2.0 $\pm$ 1.0	2.0 $\pm$ 1.0	1.0 $\pm$ 0.9
$AUC_{0 \rightarrow \infty}$ (ng·h/mL)	553.2 $\pm$ 311.9	1097.6 $\pm$ 369.7	1250.7 $\pm$ 526.4	2747.1 $\pm$ 948.7	1962.6 $\pm$ 1137.9	1361.2 $\pm$ 744.6
$t_{1/2}$ (h)	3.5 $\pm$ 1.1	2.8 $\pm$ 0.6	1.9 $\pm$ 0.3	2.1 $\pm$ 0.2	2.2 $\pm$ 1.1	2.2 $\pm$ 1.5
$F_{RB}$ (%)	100.0%	198.4%	226.1%	496.6%	354.8%	246.1%

Each point is shown as mean  $\pm$  standard deviation ( $n = 3-5$ ). Abbreviations: Sol, solution; LB<sup>SNENP</sup>, lecithin-based self-nanoemulsifying nanoemulsion preconcentrate; ir, irinotecan; ra, rapamycin; sily, silymarin; number is dose;  $F_{RB}$ , relative bioavailability.

**Table 8.** PK parameter estimations of SN38 after oral administration with Sol<sub>ir10</sub>, LBSNENP<sub>ir10</sub>, LBSNENP<sub>ir10/ra5</sub>, LBSNENP<sub>ir10/ra10</sub>, LBSNENP<sub>ir10/ra5/sily20</sub>, and LBSNENP<sub>ir10/ra10/sily20</sub>.

Title	Sol		LBSNENP			
	ir10	ir10	ir10/ra5	ir10/ra10	ir10/ra5/sily20	ir10/ra10/sily20
C <sub>max</sub> (ng/mL)	21.6 ± 3.4	141.6 ± 112.0	193.4 ± 112.2	357.7 ± 284.3	161.5 ± 125.0	202.0 ± 308.6
T <sub>max</sub> (h)	1.5 ± 0.7	0.8 ± 0.4	1.3 ± 1.4	1.5 ± 0.7	1.4 ± 0.8	1.0 ± 0.7
AUC <sub>0→∞</sub> (ng·h/mL)	137.9 ± 99.1	209.4 ± 121.9	412.1 ± 220.2	1136.5 ± 815.9	502.6 ± 333.7	684.5 ± 553.1
t <sub>1/2</sub> (h)	4.0 ± 2.1	1.9 ± 0.6	1.1 ± 0.2	1.1 ± 0.7	2.3 ± 1.6	1.2 ± 0.4
F <sub>RB</sub> (%)	100.0%	151.8%	298.8%	824.1%	364.5%	496.4%
CE (%)	37.3%	28.5%	49.3%	61.9%	38.3%	75.2%

Each point is shown as mean ± standard deviation (n = 3–5). Abbreviations: Sol, solution; LBSNENP, lecithin-based self-nanoemulsifying nanoemulsion concentrate; ir, irinotecan; ra, rapamycin; sily, silymarin; number is dose; F<sub>RB</sub>, relative bioavailability; CE, conversion efficiency.

**Table 9.** PK parameter estimation of SN38G after oral administration with Sol<sub>ir10</sub>, LBSNENP<sub>ir10</sub>, LBSNENP<sub>ir10/ra5</sub>, LBSNENP<sub>ir10/ra10</sub>, LBSNENP<sub>ir10/ra5/sily20</sub>, and LBSNENP<sub>ir10/ra10/sily20</sub>.

Title	Sol		LBSNENP			
	ir10	ir10	ir10/ra5	ir10/ra10	ir10/ra5/sily20	ir10/ra10/sily20
C <sub>max</sub> (ng/mL)	245.1 ± 117.1	454.5 ± 302.0	708.8 ± 318.5	985.7 ± 518.7	491.9 ± 204.0	789.2 ± 636.1
T <sub>max</sub> (h)	0.4 ± 0.2	0.7 ± 0.4	2.3 ± 0.6	2.3 ± 1.0	2.3 ± 1.3	1.2 ± 0.8
AUC <sub>0→∞</sub> (ng·h/mL)	2369.0 ± 652.8	3546.7 ± 1014.1	3729.3 ± 172.6	4359.9 ± 2547.8	3262.7 ± 1472.8	4058.6 ± 1718.4
t <sub>1/2</sub> (h)	5.2 ± 1.7	7.0 ± 2.1	5.1 ± 0.8	3.0 ± 0.4	4.7 ± 1.2	3.7 ± 0.7

Each point is shown as mean ± standard deviation (n = 3–5). Abbreviations: Sol, solution; LBSNENP, lecithin-based self-nanoemulsifying nanoemulsion concentrate; ir, irinotecan; ra, rapamycin; sily, silymarin; number is dose.

**Table 10.** PK parameter estimations of rapamycin after oral administration with Sol<sub>ra10</sub>, LBSNENP<sub>ra10</sub>, LBSNENP<sub>ir10/ra5</sub>, LBSNENP<sub>ir10/ra10</sub>, LBSNENP<sub>ir10/ra5/sily20</sub>, and LBSNENP<sub>ir10/ra10/sily20</sub>.

Title	Sol		LBSNENP			
	ra10	ra10	ir10/ra5	ir10/ra10	ir10/ra5/sily20	ir10/ra10/sily20
C <sub>max</sub> (ng/mL)	113.6 ± 26.4	1185.6 ± 604.2	747.4 ± 441.8	1107.1 ± 308.0	344.4 ± 37.6	1140.9 ± 863.7
T <sub>max</sub> (h)	3.3 ± 2.3	2.5 ± 0.7	2.3 ± 0.6	2.3 ± 1.0	1.8 ± 0.4	1.5 ± 0.6
AUC <sub>0→∞</sub> (ng·h/mL)	1689.5 ± 176.1	7304.0 ± 4835.6	4308.2 ± 1970.9	6598.2 ± 1092.2	2767.6 ± 700.6	6499.4 ± 2306.1
t <sub>1/2</sub> (h)	6.1 ± 3.9	4.3 ± 0.8	6.6 ± 1.9	3.4 ± 1.2	7.7 ± 4.4	4.8 ± 3.2
F <sub>RB</sub> (%)	100.0%	432.3%	255.0%	390.5%	163.8%	384.7%

Each point is shown as mean ± standard deviation (n = 3–5). Abbreviations: Sol, solution; LBSNENP, lecithin-based self-nanoemulsifying nanoemulsion concentrate; ir, irinotecan; ra, rapamycin; sily, silymarin; number is dose; F<sub>RB</sub>, relative bioavailability.

### 3.5. In Vivo Therapeutic Studies

The in vivo tumor inhibition studies of the multiple drugs loaded in LBSNENP were performed using a nude mouse model bearing MIA PaCa-2 xenografts. The tumor growth curves are illustrated in Figure 3A. After the oral administration of all the formulations was performed four times, except in the control group (saline), the treatment groups exhibited substantial inhibition in the growth of MIA PaCa-2 cells. The TGI% on day 12 for LBSNENP<sub>ir10/ra10/sily20</sub> was 88.4%. The TGI% on day 12 was 84.3%, 80.0%, 71.9%, 82.8%, and 79.8% for LBSNENP<sub>ir10/ra5/sily20</sub>, LBSNENP<sub>ir10</sub>, LBSNENP<sub>ra10</sub>, LBSNENP<sub>ir10/ra10</sub>, and LBSNENP<sub>ir10/ra5</sub>, respectively. At the same dose of irinotecan combined with rapamycin, LBSNENP<sub>ir10/ra10/sily20</sub> and LBSNENP<sub>ir10/ra5/sily20</sub> exhibited greater antitumor activity than

that of dual drugs ( $\text{LB-SNENP}_{\text{ir}10/\text{ra}10}$  and  $\text{LB-SNENP}_{\text{ir}10/\text{ra}5}$ ). During the regular observation period (every 3 days), the tumor growth rate was slower in the treatment group of  $\text{LB-SNENP}_{\text{ir}10/\text{ra}10/\text{sily}20}$  than in the other groups after the last administration. On day 31, we sacrificed the mice through  $\text{CO}_2$  inhalation, and the tumors were harvested and weighed. Figure 3B illustrates the excised tumor mass. Significant differences in tumor weights were observed between the combination and control groups ( $p < 0.05$ ). During the 30-day experimental period, changes were observed in the mouse weight across each experimental group. These are shown in Figure 3C. The treatment groups exhibited a slight weight loss of not more than 20%. The survival rate is presented in Figure 3D. One mouse in the  $\text{LB-SNENP}_{\text{ir}10/\text{ra}10/\text{sily}20}$  group died on day 6, and one mouse in the  $\text{LB-SNENP}_{\text{ir}10/\text{ra}10}$  group died on day 9. Diarrhea is a severe side effect of irinotecan. No diarrhea was noted in the nude mice in all the experimental groups. These results indicate that  $\text{LB-SNENP}$ -encapsulated irinotecan, rapamycin, and silymarin not only reduced the dose of the drugs to achieve treatment efficacy but also considerably reduced side effects.

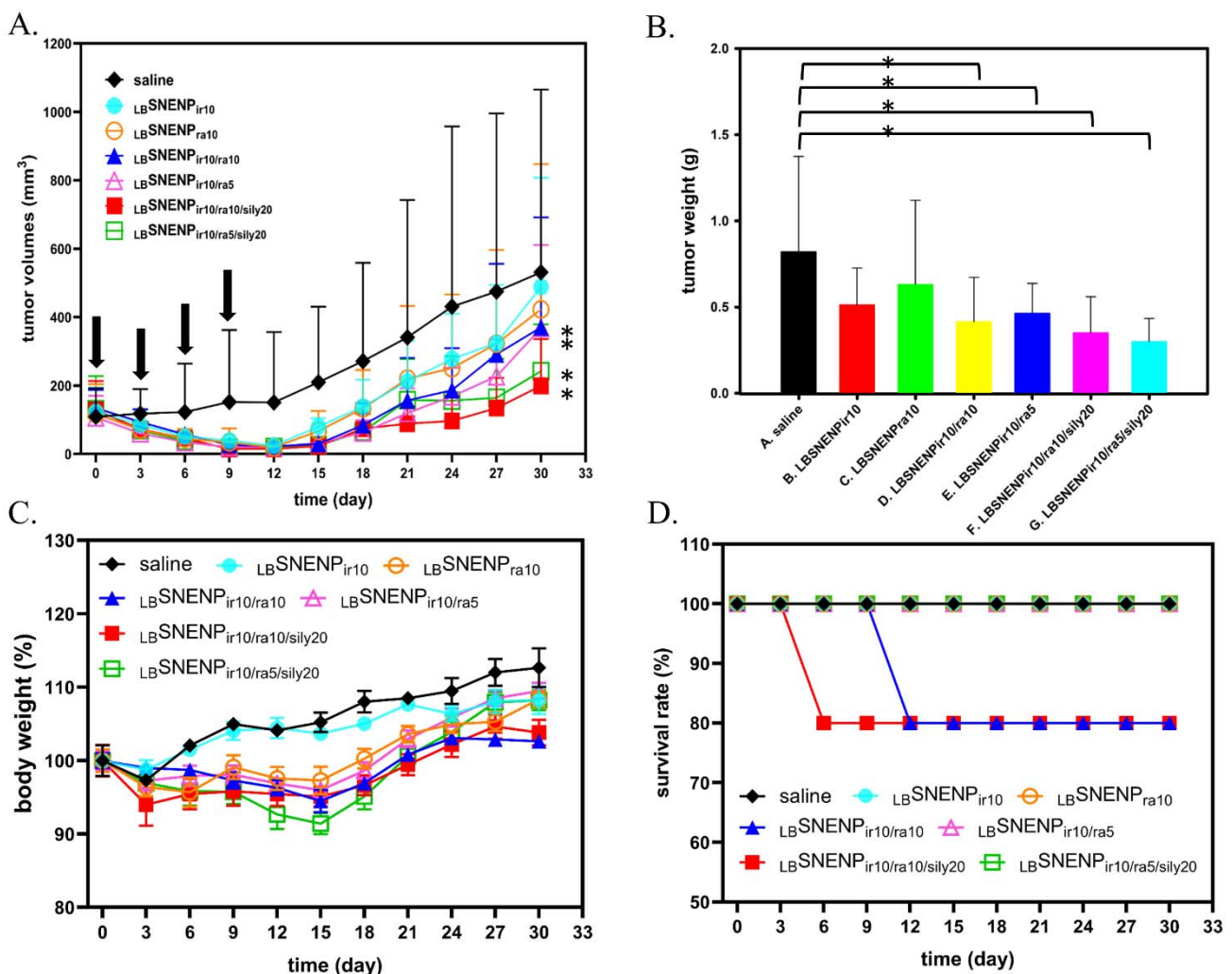


**Figure 3.** Tumor inhibition studies (A); tumor weight (B); body weight changes (C); and survival rate (D) of nude mice bearing Mia PaCa-2 tumor xenografts after oral administration with saline,  $\text{LB-SNENP}_{\text{ir}10}$ ,  $\text{LB-SNENP}_{\text{ra}10}$ ,  $\text{LB-SNENP}_{\text{ir}10/\text{ra}5}$ ,  $\text{LB-SNENP}_{\text{ir}10/\text{ra}10}$ ,  $\text{LB-SNENP}_{\text{ir}10/\text{ra}5/\text{sily}20}$ , and  $\text{LB-SNENP}_{\text{ir}10/\text{ra}10/\text{sily}20}$  (on days 0, 3, 6, and 9). Each point is shown as mean  $\pm$  standard deviation ( $n = 4$  to 5). \*  $p < 0.05$  when  $\text{LB-SNENP}_{\text{ir}10/\text{ra}5}$ ,  $\text{LB-SNENP}_{\text{ir}10/\text{ra}10}$ ,  $\text{LB-SNENP}_{\text{ir}10/\text{ra}5/\text{sily}20}$ , and  $\text{LB-SNENP}_{\text{ir}10/\text{ra}10/\text{sily}20}$  were compared with saline. Abbreviations:  $\text{LB-SNENP}$ , lecithin-based self-nanoemulsifying nanoemulsion preconcentrate; ir, irinotecan; ra, rapamycin; sily, silymarin; number is dose.

#### 4. Conclusions

In this study, we successfully developed an oral lecithin-based self-nanoemulsifying nanoemulsion drug delivery system ( $_{LB}SNENA$ ), which could simultaneously encapsulate one or more hydrophobic drugs to improve their solubility and oral bioavailability. This drug delivery system had a nanoscale particle size and high stability. Furthermore, the *in vivo* and *in vitro* studies of irinotecan, rapamycin, and silymarin loaded in  $_{LB}SNENP$  exhibited their significant anticancer synergistic effects on human pancreatic cancer cells. The combination of multiple drugs with different pharmacological mechanisms considerably increased the inhibition of tumor proliferation, reduced the dosage of a single drug, and prevented the occurrence of side effects. Thus, irinotecan combined with rapamycin and silymarin, loaded in  $_{LB}SNENP$  to form a self-nanoemulsifying nanoemulsion, is a potential drug delivery system for the oral administration of chemotherapy drugs and exerts synergistic antitumor effects.

**Supplementary Materials:** The following supporting information can be downloaded at: <https://www.mdpi.com/article/10.3390/pharmaceutics15020473/s1>, Figure S1: Analytical graphs of HPLC: (A) irinotecan, and (B) rapamycin; Figure S2: Analytical graphs of LCMS.

**Author Contributions:** Conceptualization, writing—review and editing and project administration: H.-O.H. and H.-L.L.; methodology, software, validation, formal analysis and writing—original draft preparation: Y.-H.L., L.-C.C. and W.-T.C.; investigation, data curation and visualization: P.-S.W. and C.-M.H.; resources, supervision and funding acquisition: M.-T.S. and S.-Y.L. All authors have read and agreed to the published version of the manuscript.

**Funding:** This study was partially supported by research grants from the Ministry of Science and Technology of the Republic of China (MOST 111-2221-E-037-004) and Jin-lung-yuan Foundation (2022–2023).

**Institutional Review Board Statement:** This animal experiment was approved by the Institutional Animal Care and Use Committee of Taipei Medical University (Approval No.: LAC-2017-0334) in compliance with the Taiwanese Animal Welfare Act.

**Informed Consent Statement:** Not applicable.

**Data Availability Statement:** Source data are available from the corresponding author upon reasonable request.

**Acknowledgments:** The authors acknowledge the technical support provided by TMU Core Facility.

**Conflicts of Interest:** The funders had no role in the design of the study; in the collection, analyses, or interpretation of data; in the writing of the manuscript; or in the decision to publish the results.

#### References

1. Kamisawa, T.; Wood, L.D.; Itoi, T.; Takaori, K. Pancreatic cancer. *Lancet* **2016**, *388*, 73–85. [[CrossRef](#)] [[PubMed](#)]
2. Siegel, R.L.; Miller, K.D.; Jemal, A. Cancer statistics, 2019. *CA Cancer J. Clin.* **2019**, *69*, 7–34. [[CrossRef](#)] [[PubMed](#)]
3. Gillen, S.; Schuster, T.; Meyer Zum Büschenfelde, C.; Friess, H.; Kleeff, J. Preoperative/neoadjuvant therapy in pancreatic cancer: A systematic review and meta-analysis of response and resection percentages. *PLoS Med.* **2010**, *7*, e1000267. [[CrossRef](#)]
4. Conroy, T.; Desseigne, F.; Ychou, M.; Bouché, O.; Guimbaud, R.; Bécouarn, Y.; Adenis, A.; Raoul, J.L.; Gourgou-Bourgade, S.; de la Fouchardière, C.; et al. FOLFIRINOX versus gemcitabine for metastatic pancreatic cancer. *N. Engl. J. Med.* **2011**, *364*, 1817–1825. [[CrossRef](#)] [[PubMed](#)]
5. Von Hoff, D.D.; Ervin, T.; Arena, F.P.; Chiorean, E.G.; Infante, J.; Moore, M.; Seay, T.; Tjulandin, S.A.; Ma, W.W.; Saleh, M.N.; et al. Increased survival in pancreatic cancer with nab-paclitaxel plus gemcitabine. *N. Engl. J. Med.* **2013**, *369*, 1691–1703. [[CrossRef](#)]
6. Wang, J.P.; Wu, C.Y.; Yeh, Y.C.; Shyr, Y.M.; Wu, Y.Y.; Kuo, C.Y.; Hung, Y.P.; Chen, M.H.; Lee, W.P.; Luo, J.C.; et al. Erlotinib is effective in pancreatic cancer with epidermal growth factor receptor mutations: A randomized, open-label, prospective trial. *Oncotarget* **2015**, *6*, 18162–18173. [[CrossRef](#)]
7. Morran, D.C.; Wu, J.; Jamieson, N.B.; Mrowinska, A.; Kalna, G.; Karim, S.A.; Au, A.Y.; Scarlett, C.J.; Chang, D.K.; Pajak, M.Z.; et al. Targeting mTOR dependency in pancreatic cancer. *Gut* **2014**, *63*, 1481–1489. [[CrossRef](#)]
8. Zhong, H.; Chiles, K.; Feldser, D.; Laughner, E.; Hanrahan, C.; Georgescu, M.M.; Simons, J.W.; Semenza, G.L. Modulation of hypoxia-inducible factor 1 $\alpha$  expression by the epidermal growth factor/phosphatidylinositol 3-kinase/PTEN/AKT/FRAP pathway in human prostate cancer cells: Implications for tumor angiogenesis and therapeutics. *Cancer Res.* **2000**, *60*, 1541–1545.

9. Forsythe, J.A.; Jiang, B.H.; Iyer, N.V.; Agani, F.; Leung, S.W.; Koos, R.D.; Semenza, G.L. Activation of vascular endothelial growth factor gene transcription by hypoxia-inducible factor 1. *Mol. Cell Biol.* **1996**, *16*, 4604–4613. [[CrossRef](#)]
10. Büchler, P.; Reber, H.A.; Lavey, R.S.; Tomlinson, J.; Büchler, M.W.; Friess, H.; Hines, O.J. Tumor hypoxia correlates with metastatic tumor growth of pancreatic cancer in an orthotopic murine model. *J. Surg. Res.* **2004**, *120*, 295–303. [[CrossRef](#)]
11. Liu, Y.; Feng, M.; Chen, H.; Yang, G.; Qiu, J.; Zhao, F.; Cao, Z.; Luo, W.; Xiao, J.; You, L.; et al. Mechanistic target of rapamycin in the tumor microenvironment and its potential as a therapeutic target for pancreatic cancer. *Cancer Lett.* **2020**, *485*, 1–13. [[CrossRef](#)] [[PubMed](#)]
12. Vaupel, P. The role of hypoxia-induced factors in tumor progression. *Oncologist* **2004**, *9* (Suppl. 5), 10–17. [[CrossRef](#)] [[PubMed](#)]
13. Semenza, G.L. Defining the role of hypoxia-inducible factor 1 in cancer biology and therapeutics. *Oncogene* **2010**, *29*, 625–634. [[CrossRef](#)] [[PubMed](#)]
14. Abou Khouzam, R.; Brodaczewska, K.; Filipiak, A.; Zeinelabdin, N.A.; Buart, S.; Szczylik, C.; Kieda, C.; Chouaib, S. Tumor Hypoxia Regulates Immune Escape/Invasion: Influence on Angiogenesis and Potential Impact of Hypoxic Biomarkers on Cancer Therapies. *Front. Immunol.* **2020**, *11*, 613114. [[CrossRef](#)]
15. Pencreach, E.; Guérin, E.; Nicolet, C.; Lelong-Rebel, I.; Voegeli, A.C.; Oudet, P.; Larsen, A.K.; Gaub, M.P.; Guenot, D. Marked activity of irinotecan and rapamycin combination toward colon cancer cells in vivo and in vitro is mediated through cooperative modulation of the mammalian target of rapamycin/hypoxia-inducible factor-1alpha axis. *Clin. Cancer Res.* **2009**, *15*, 1297–1307. [[CrossRef](#)]
16. Forster, R.E.; Tang, Y.; Bowyer, C.; Lloyd, A.W.; Macfarlane, W.; Phillips, G.J.; Lewis, A.L. Development of a combination drug-eluting bead: Towards enhanced efficacy for locoregional tumour therapies. *Anticancer Drugs* **2012**, *23*, 355–369. [[CrossRef](#)]
17. Jannier, S.; Kemmel, V.; Sebastia Sancho, C.; Chammas, A.; Sabo, A.N.; Pencreach, E.; Farace, F.; Chenard, M.P.; Lhermitte, B.; Georger, B.; et al. SFCE-RAPIRI Phase I Study of Rapamycin Plus Irinotecan: A New Way to Target Intra-Tumor Hypoxia in Pediatric Refractory Cancers. *Cancers* **2020**, *12*, 3051. [[CrossRef](#)] [[PubMed](#)]
18. Suzuki, K.; Takeuchi, O.; Suzuki, Y.; Kitagawa, Y. Mechanisms of metformin's anti-tumor activity against gemcitabine-resistant pancreatic adenocarcinoma. *Int. J. Oncol.* **2019**, *54*, 764–772. [[CrossRef](#)]
19. Veltkamp, S.A.; Thijssen, B.; Garrigue, J.S.; Lambert, G.; Lallemand, F.; Binlich, F.; Huitema, A.D.; Nuijen, B.; Nol, A.; Beijnen, J.H.; et al. A novel self-microemulsifying formulation of paclitaxel for oral administration to patients with advanced cancer. *Br. J. Cancer* **2006**, *95*, 729–734. [[CrossRef](#)]
20. Goodin, S. Oral chemotherapeutic agents: Understanding mechanisms of action and drug interactions. *Am. J. Health Syst. Pharm.* **2007**, *64*, S15–S24. [[CrossRef](#)]
21. Sparreboom, A.; van Asperen, J.; Mayer, U.; Schinkel, A.H.; Smit, J.W.; Meijer, D.K.; Borst, P.; Nooijen, W.J.; Beijnen, J.H.; van Tellingen, O. Limited oral bioavailability and active epithelial excretion of paclitaxel (Taxol) caused by P-glycoprotein in the intestine. *Proc. Natl. Acad. Sci. USA* **1997**, *94*, 2031–2035. [[CrossRef](#)] [[PubMed](#)]
22. Yang, S.; Gursoy, R.N.; Lambert, G.; Benita, S. Enhanced oral absorption of paclitaxel in a novel self-microemulsifying drug delivery system with or without concomitant use of P-glycoprotein inhibitors. *Pharm. Res.* **2004**, *21*, 261–270. [[CrossRef](#)] [[PubMed](#)]
23. Chen, L.C.; Cheng, W.J.; Lin, S.Y.; Hung, M.T.; Sheu, M.T.; Lin, H.L.; Hsieh, C.M. CPT11 with P-glycoprotein/CYP 3A4 dual-function inhibitor by self-nanoemulsifying nanoemulsion combined with gastroretentive technology to enhance the oral bioavailability and therapeutic efficacy against pancreatic adenocarcinomas. *Drug Deliv.* **2021**, *28*, 2205–2217. [[CrossRef](#)] [[PubMed](#)]
24. Lin, H.L.; Chen, L.C.; Cheng, W.T.; Cheng, W.J.; Ho, H.O.; Sheu, M.T. Preparation and Characterization of a Novel Swellable and Floating Gastroretentive Drug Delivery System (sfGRDDS) for Enhanced Oral Bioavailability of Nilotinib. *Pharmaceutics* **2020**, *12*, 137. [[CrossRef](#)]
25. Lin, Y.M.; Wu, J.Y.; Chen, Y.C.; Su, Y.D.; Ke, W.T.; Ho, H.O.; Sheu, M.T. In situ formation of nanocrystals from a self-microemulsifying drug delivery system to enhance oral bioavailability of fenofibrate. *Int. J. Nanomed.* **2011**, *6*, 2445–2457. [[CrossRef](#)]
26. Lin, S.F.; Chen, Y.C.; Ho, H.O.; Huang, W.Y.; Sheu, M.T.; Liu, D.Z. Development and characterization of dilutable self-microemulsifying premicroemulsion systems (SMEPMS) as templates for preparation of nanosized particulates. *Int. J. Nanomed.* **2013**, *8*, 3455–3466. [[CrossRef](#)]
27. Chen, L.C.; Chen, Y.C.; Su, C.Y.; Hong, C.S.; Ho, H.O.; Sheu, M.T. Development and characterization of self-assembling lecithin-based mixed polymeric micelles containing quercetin in cancer treatment and an in vivo pharmacokinetic study. *Int. J. Nanomed.* **2016**, *11*, 1557–1566. [[CrossRef](#)]
28. Su, C.Y.; Liu, J.J.; Ho, Y.S.; Huang, Y.Y.; Chang, V.H.; Liu, D.Z.; Chen, L.C.; Ho, H.O.; Sheu, M.T. Development and characterization of docetaxel-loaded lecithin-stabilized micellar drug delivery system (L(sb)MDDs) for improving the therapeutic efficacy and reducing systemic toxicity. *Eur. J. Pharm. Biopharm.* **2018**, *123*, 9–19. [[CrossRef](#)] [[PubMed](#)]
29. Pawarode, A.; Minderman, H.; O'loughlin, K.L.; Greco, W.R.; Baer, M.R. Rapamycin overcomes multidrug resistance (MDR) mediated by P-glycoprotein (Pgp), Multidrug Resistance Protein-1 (MRP-1), Breast Cancer Resistance Protein (BCRP) and Lung Resistance Protein (LRP) and synergizes with substrate drugs in MDR cells. *Cancer Res.* **2006**, *66*, 1270.

30. Si, J.; Zhao, X.; Gao, S.; Huang, D.; Sui, M. Advances in delivery of Irinotecan (CPT-11) active metabolite 7-ethyl-10-hydroxycamptothecin. *Int. J. Pharm.* **2019**, *568*, 118499. [[CrossRef](#)] [[PubMed](#)]
31. Du, Z.; Wang, G.; Cao, Y.F.; Hu, C.M.; Yang, K.; Liu, Y.Z.; Zhang, C.Z.; Zhang, W.H.; Zhu, Z.T.; Sun, H.Z.; et al. Everolimus-inhibited multiple isoforms of UDP-glucuronosyltransferases (UGTs). *Xenobiotica* **2018**, *48*, 452–458. [[CrossRef](#)] [[PubMed](#)]

**Disclaimer/Publisher's Note:** The statements, opinions and data contained in all publications are solely those of the individual author(s) and contributor(s) and not of MDPI and/or the editor(s). MDPI and/or the editor(s) disclaim responsibility for any injury to people or property resulting from any ideas, methods, instructions or products referred to in the content.